Technical University of Denmark

Regional frequency analysis of short duration rainfall extremes using gridded daily rainfall data as co-variate

Madsen, H.; Gregersen, Ida Bülow; Rosbjerg, Dan; Arnbjerg-Nielsen, Karsten

Published in:
Water Science and Technology

Link to article, DOI:
10.2166/wst.2017.089

Publication date:
2017

Document Version
Peer reviewed version

REGIONAL FREQUENCY ANALYSIS OF SHORT DURATION RAINFALL EXTREMES USING GRIDDED DAILY RAINFALL DATA AS CO-VARIATE

Short title: Regional frequency analysis of short duration rainfall extremes

H. Madsen[(1)*], I.B. Gregersen[(2)], D. Rosbjerg[(2)], K. Arnbjerg-Nielsen[(2)]

[(1)] *DHI, Agern Allé 5, DK-2970 Hørsholm, Denmark*

[(2)] *Technical University of Denmark, Department of Environmental Engineering, Bygningstorvet Building 115, DK-2800 Kgs. Lyngby, Denmark*

[*] Corresponding author. E-mail: hem@dhigroup.com

ABSTRACT

A regional partial duration series (PDS) model is applied for estimation of intensity duration frequency relationships of extreme rainfalls in Denmark. The model uses generalised least squares regression to relate the PDS parameters to gridded rainfall statistics from a dense network of rain gauges with daily measurements. The Poisson rate is positively correlated to the mean annual precipitation for all durations considered (1 min to 48 hours). The mean intensity can be assumed constant over Denmark for durations up to 1 hour. For durations larger than 1 hour the mean intensity is significantly correlated to the mean extreme daily precipitation. A Generalised Pareto distribution with a regional constant shape parameter is adopted. Compared to previous regional studies in Denmark a general increase in extreme rainfall intensity for durations up to 1 hour is found, whereas for larger durations both increases and decreases are seen. A subsample analysis is conducted to evaluate the impacts of non-stationarities in the rainfall data. The regional model includes the non-stationarities as an additional source of uncertainty together with sampling uncertainty and uncertainty caused by spatial variability.

KEYWORDS: extreme rainfall, idf-curves, L-moments, partial duration series, regional analysis

INTRODUCTION

Design of water infrastructure is often based on intensity duration frequency (IDF) relationships of extreme rainfall (e.g. Schilling, 1991; Arnbjerg-Nielsen *et al.*, 2013). They provide information about the mean rainfall intensity of different durations for various frequencies or return periods. IDF relationships are relevant for a wide range of temporal scales; from sub-hourly duration for design of storm water pipes in the upstream parts of sewer networks to several hours or days for design of retention basins that collect water from large catchments. IDF relationships can be estimated by performing an extreme value analysis of rainfall data at the site of interest. Such estimates, however, may be hampered by the lack of sufficiently long rainfall records when extrapolating to large return periods. In regional frequency analysis data from several sites within a region are pooled whereby the estimation uncertainty can be reduced significantly (e.g. Madsen & Rosbjerg, 1997a; Kyselý *et al.*, 2011; Burn, 2014). In addition, regional frequency analysis facilitates estimation of IDF relationships at ungauged sites by combining regional extreme value statistics and site specific climatic and physiographic characteristics.

A widely applied method in regional frequency analysis is the index-event approach (originally named the index-flood approach in flood frequency analysis) using L-moments (Hosking & Wallis, 1993; 1997). This approach has been used in several regional frequency analysis studies of extreme rainfall, e.g. in Australia (Haddad *et al.*, 2011), Canada (Alila, 1999; Burn, 2014), Czech Republic (Kyselý *et al.*, 2011), Italy (Di Baldassarre *et al.*, 2006), Slovakia (Gaál *et al.*, 2008), South Africa (Smithers & Schulze, 2001), and Washington State (Wallis *et al.*, 2007). All these studies are based on the traditional index-event method using annual maximum series (AMS). Madsen & Rosbjerg (1997a) developed a regional index-event approach based on Partial Duration Series (PDS) that includes all events above a specified threshold level in the extreme value analysis. Madsen *et al.* (1997) showed that the regional index-event PDS model with generalized Pareto distributed exceedances, in general, is more efficient (in terms of quantile estimation uncertainty) than the corresponding index-event AMS model based on the generalized extreme value distribution. The regional PDS model has been further developed and applied for estimation of IDF relationships in Denmark (Madsen *et al.*, 2002; 2009).

In the traditional index-event approach data are pooled within a fixed region that can be assumed to be homogenous with respect to certain statistical characteristics, typically second and higher order moments. Alternatively, a region of influence approach can be used to identify separate homogeneous pooling groups for each site (Burn, 1990). The region of influence approach has been applied to regional rainfall analysis by Kyselý *et al.* (2011) and Burn (2014). Another method that relaxes the use of fixed regions, or can be used in combination with a fixed region or region of influence approach, is based on establishing regression relationships that describe the spatial variation of extreme rainfall statistics using covariate information in terms of physiographic and climatic characteristics. Such regional regression relationships also facilitate estimation at ungauged sites. In a regional analysis in Washington State, Wallis *et al.* (2007) found the L-Coefficient of variation (L-CV) and L-skewness to vary systematically with the mean annual precipitation (MAP). Di Baldassarre *et al.* (2006) also related L-CV and L-Skewness to MAP in their study of rainfall extremes in Northern Italy, and Madsen *et al.* (2002, 2009) found that the annual number of extreme events in a regional PDS model of Danish rainfall extremes could be related to MAP. Haddad *et al.* (2011) related L-CV and L-skewness as well as the index parameter to location and distance to the coast, whereas Beguería & Vicente-Serrano (2006) applied a regional regression model relating the PDS parameters to location, altitude and slope.

This study considers regional estimation of IDF relationships in Denmark. It builds on the regional PDS model developed by Madsen *et al.* (2002) and later updated by Madsen *et al.* (2009). The current study includes rainfall data up to 2012, corresponding to 50% more data in terms of station-years compared to the previous study by Madsen *et al.* (2009). In addition, the regional model is extended by using new covariate information in terms of gridded rainfall statistics from a dense rain gauge network measuring daily rainfall. In the update of the regional model by Madsen *et al.* (2009) a general increase in extreme rainfall was found, with most pronounced increases for durations between 10 min and 3 hours. In a recent study by Gregersen *et al.* (2013) a significant increase was found in the annual number of extreme events for all durations analysed between 1 and 24 hours and in the mean extreme intensity for 1 and 3-hour durations. In this study, the impacts of these non-stationarities on the regional model are investigated using subsample analysis.

DATA AND METHODS

Rainfall data

Rainfall data from a network of high-resolution rain gauges in Denmark are used in the analysis. The network is based on RIMCO tipping bucket gauges with 0.2 mm resolution and tips being recorded every minute. The network was established in 1979 and is operated by the Water Pollution Committee of the Society of Danish Engineers and the Danish Meteorological Institute (Jørgensen *et al.*, 1998). The gauges have been maintained, but the principles of measuring and calibrating the gauges have not been changed in the period investigated.

The data analysed consist of rainfall intensities with a temporal resolution of 1 minute for individual rain events separated by dry periods of at least one hour. From the 1-minute intensity data maximum rainfall intensities for durations ranging between 1 minute and 48 hours are extracted using a moving window approach (Madsen et al., 2002). For durations less than one hour, independent events are separated by at least one hour dry periods. For durations larger than one hour, independent events are separated by dry periods that are at least as large as the duration considered. In this case the separate events defined for the 1-minute intensity data will be merged into fewer and larger independent events. For the extreme value analysis Partial Duration Series (PDS) are derived for each duration from the series of event-based maximum intensities by including intensities above a pre-defined threshold level. The same threshold levels as applied in the previous analyses (Madsen *et al.*, 2002; 2009) are used. Short-duration (less than 1-2 hours) extremes are primarily caused by convective rainfall in summer months, whereas long-duration (larger than 12-24 hours) extremes are caused by frontal rainfall and can occur all year round.

Rainfall data used in the analysis cover the period 1 January 1979 – 31 December 2012 and include 83 stations with more than 10 years of observations. The location of the 83 stations is shown in Supplementary Material Figure 1, and the distribution of observation periods is shown in Figure 1. The dataset corresponds to a total of 1881 station-years. The earlier study by Madsen *et al.* (2009) included 66 stations with a total of 1250 station-years, and hence the current study comprises an increase in station-years of 50%.

The development of the annual number of station-years shows a relatively constant level of about 40 station-years per year up to 1990, followed by a steady increase up to a level of about 70 station-years per year during the last 10 years (see Figure 1). To evaluate the impact of the development in data availability over time a subsample of 31 stations that have more than 30 years of observations is analysed. The subsample includes 999 station-years in total.

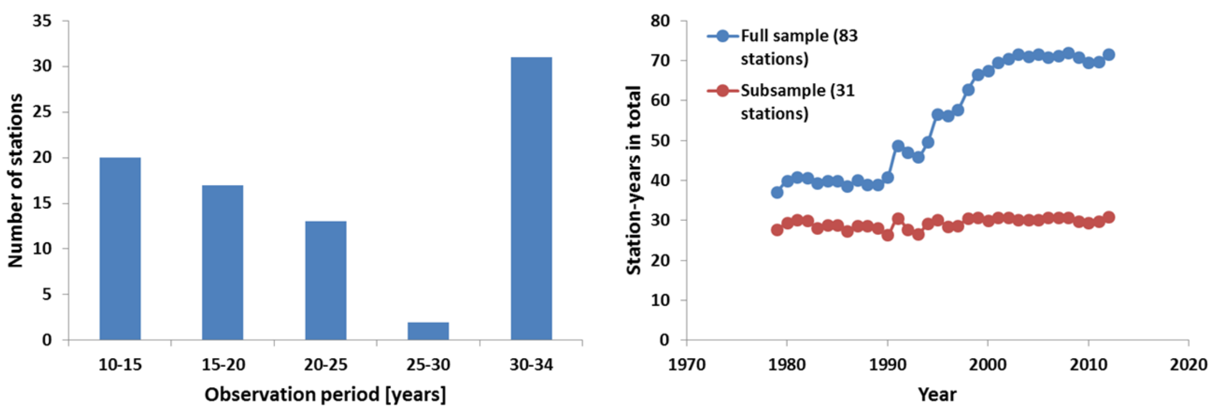

Figure 1 Distribution of observation periods of the 83 stations included in the analysis (left), and development of the annual number of station-years during the period 1979-2012 for, respectively, the full sample of 83 stations and the subsample consisting of the 31 stations with more than 30 years of data (right).

In the regional model covariate information from another precipitation dataset, the Climate Grid Denmark (CGD), is used. CGD is a gridded dataset of daily precipitation prepared by the Danish Meteorological Institute (Scharling, 2012). It has a spatial resolution of 10x10 km and covers the period 1989-2010. The dataset is based on interpolation of rain gauge measurements from more than 300 Hellman gauges using an inverse distance weighting approach (Scharling, 1999). From the CGD dataset the mean annual precipitation and the mean extreme daily precipitation are calculated. The mean annual precipitation (MAP) varies between 550 and 950 mm over Denmark with the highest values in the Western part of the country (see Figure 3). The mean extreme daily precipitation (μ_{CGD}) is estimated from the CGD data using a PDS model with a regional constant threshold level corresponding to approximately three events per year. It varies between 24.5 and 29.5 mm over Denmark with larger values in eastern Zealand, northern Jutland and southern islands (see Figure 3).

In the previous studies by Madsen *et al.* (2002, 2009) different physiographic characteristics (geographical location, altitude, shelter index) were included as covariates in the regression analysis. However, none of these were found significant for describing the regional variability and hence are not included in this study.

Regional model

The regional extreme value model developed by Madsen *et al.* (2002) is applied in this study. The model is based on the PDS approach using a regional constant threshold level to define PDS of extreme rainfall intensities at the different stations. In the regional PDS model the annual number of extreme events is assumed to follow a Poisson distribution, and the magnitude of the extreme events is assumed to follow a Generalised Pareto (GP) distribution. For determination of a regional parent distribution the previous studies by Madsen *et al.* (2002, 2009) applied the L-moment goodness-of-fit test proposed by Hosking & Wallis (1993) and extended by Madsen *et al.* (2002) for application to two-parameter distributions used in PDS modelling. These studies showed that the GP distribution was, in general, preferable for the range of rainfall durations considered.

In the regional PDS model the Poisson rate (λ), and the mean (μ) and L-CV (τ_2) of the exceedance magnitudes are modelled as regional variables. The regional model estimate of the rainfall intensity for a given return period T is then given by (Madsen *et al.*, 2002)

$$\hat{z}_T = z_0 + \hat{\mu}\frac{1+\hat{\kappa}}{\hat{\kappa}}\left[1-\left(\frac{1}{\hat{\lambda}T}\right)^{\hat{\kappa}}\right] \ ,\hat{\kappa} = \frac{1}{\hat{\tau}_2} - 2 \qquad (1)$$

where z_0 is the regional threshold level, $\hat{\lambda}$, $\hat{\mu}$, and $\hat{\tau}_2$ are regional model estimates of the Poisson rate, mean, and L-CV, respectively, and $\hat{\kappa}$ is the corresponding estimate of the GP shape parameter.

The regional variability of the PDS parameters are analysed using generalised least squares (GLS) regression (Stedinger & Tasker, 1985; Madsen & Rosbjerg, 1997b). The GLS regression model accounts for sampling uncertainties of the PDS parameter estimates as well as correlations between the parameter estimates due to concurrent extreme events observed at different stations in the region. The following regression model is considered

$$\hat{\theta}_i = \beta_0 + \sum_{k=1}^{p}\beta_k x_{ki} + \omega_i \quad ,i = 1,2,..,M \qquad (2)$$

where $\hat{\theta}_i$ denotes an estimate of one of the PDS parameters at station *i*, *M* is the number of stations, β_k are the regression parameters, x_{ki} are the covariates, and ω_i are the model residuals with covariance matrix

$$\Sigma = \begin{pmatrix} \sigma_{\varepsilon 1}^2 + \sigma_\delta^2 & \sigma_{\varepsilon 1}\sigma_{\varepsilon 2}\rho_{12} & \cdots & \sigma_{\varepsilon 1}\sigma_{\varepsilon M}\rho_{1M} \\ \sigma_{\varepsilon 2}\sigma_{\varepsilon 1}\rho_{12} & \sigma_{\varepsilon 2}^2 + \sigma_\delta^2 & \cdots & \sigma_{\varepsilon 2}\sigma_{\varepsilon M}\rho_{2M} \\ \vdots & & \ddots & \vdots \\ \sigma_{\varepsilon M}\sigma_{\varepsilon 1}\rho_{1M} & \sigma_{\varepsilon M}\sigma_{\varepsilon 2}\rho_{2M} & \cdots & \sigma_{\varepsilon M}^2 + \sigma_\delta^2 \end{pmatrix} \tag{3}$$

In Eq. (3), $\sigma_{\varepsilon i}^2$ is the sampling error variance, σ_δ^2 is the residual model error variance, and ρ_{ij} is the sampling error correlation coefficient. Estimation of sampling variances and correlations to be used in the GLS regression model are described in Madsen *et al.* (2002). σ_δ^2 is estimated along with the regression parameters using an iterative scheme, see Madsen & Rosbjerg (1997b) for details.

The GLS regression model provides estimates of the PDS parameters and their associated variances at any location in the region. The *T*-year estimate at a given location is then obtained from Eq. (1). The variance of the *T*-year estimate is calculated based on the variances of the PDS parameter estimates from the GLS regression models using a Taylor series approximation of Eq. (1)

$$Var\{\hat{z}_T\} = \left(\frac{\partial z_T}{\partial \lambda}\right)^2 Var\{\hat{\lambda}\} + \left(\frac{\partial z_T}{\partial \mu}\right)^2 Var\{\hat{\mu}\} + \left(\frac{\partial z_T}{\partial \kappa}\right)^2 Var\{\hat{\kappa}\} \tag{4}$$

where the partial derivatives are evaluated around the GLS parameter estimates.

The variances of the estimated PDS parameters include both residual model error variance and sampling variance corrected for intersite correlations. When only the intercept β_0 is included in the regression model, the model provides an estimate of the regional mean PDS parameter, and the estimate of the residual model error variance $\hat{\sigma}_\delta^2$ is then a measure of regional heterogeneity. The regional mean is, in general, different from the arithmetic mean since the GLS model weighs the estimated PDS parameters according to the error covariance matrix, hence giving less weight to more uncertain estimates and groups of sites that have higher inter-site correlations (Madsen and Rosbjerg, 1997b). If $\hat{\sigma}_\delta^2 = 0$, the region can be considered homogeneous and the observed variability of the PDS parameter estimates at the different sites in the region can be explained by sampling uncertainty. A residual model error variance larger than zero indicates a heterogeneous region, and one can then apply the GLS regression model with available covariate information to evaluate the potential of describing the regional variability.

Different diagnostics are applied to evaluate the GLS regression models. Madsen & Rosbjerg (1997b) used the average prediction variance of the regression model estimates $\hat{\sigma}_{\theta i}^2$ for all stations i = 1,2,…,M in the region

$$\hat{\sigma}_{\theta i}^2 = y_i^T \sum(\hat{\beta}) y_i + \hat{\sigma}_\delta^2 \qquad , y_i = (1 \;\; x_{1i} \;\; \cdots \;\; x_{pi}) \tag{5}$$

where $\sum(\hat{\beta})$ is the covariance matrix of the estimated regression parameters. The prediction variance includes both the sampling uncertainty of the estimated regression model parameters and the residual model error variance. When comparing different regression models, the model with the smallest average prediction variance is preferred. The reduction in prediction variance (*RPV*) between a regression model with k explanatory variables, $\hat{\sigma}^2_{\theta i}(k)$, and the regional mean model, $\hat{\sigma}^2_{\theta i}(0)$, can be used as a measure of the value of covariate information

$$RPV = \frac{\sum_{i=1}^{M} \hat{\sigma}^2_{\theta i}(0) - \sum_{i=1}^{M} \hat{\sigma}^2_{\theta i}(k)}{\sum_{i=1}^{M} \hat{\sigma}^2_{\theta i}(0)} = 1 - \frac{\sum_{i=1}^{M} \hat{\sigma}^2_{\theta i}(k)}{\sum_{i=1}^{M} \hat{\sigma}^2_{\theta i}(0)} \qquad (6)$$

Note that *RPV* can become negative in the case where the inclusion of explanatory variables only provides a minor reduction in residual model error variance, which is smaller than the corresponding increase in the sampling uncertainty of the estimated regression model parameters.

Reis *et al.* (2004) proposed a pseudo coefficient of determination

$$R^2 = 1 - \frac{\hat{\sigma}^2_{\delta}(k)}{\hat{\sigma}^2_{\delta}(0)} \qquad (7)$$

where $\hat{\sigma}^2_{\delta}(k)$ and $\hat{\sigma}^2_{\delta}(0)$ are the residual model error variances for, respectively, a regression model with k explanatory variables and the regional mean model. Note that if $\hat{\sigma}^2_{\delta}(k) = 0$ then R^2 = 1 although the model is not perfect. In this case sampling errors account for the differences between the site specific PDS parameter estimates and the GLS regression model estimates. Compared to *RPV*, R^2 only considers the reduction in residual model error variance by using covariate information.

Finally, the significance of the estimated regression parameters is evaluated using a standard t-test.

RESULTS

Regional model

For the Poisson rate parameter λ the GLS results show regional variability ($\hat{\sigma}_\delta^2(0) > 0$) for all durations, and a part of this variability can be explained by MAP. The GLS regression models with MAP have smaller average prediction variances than the regional mean models. *RPV* ranges between 0.01 and 0.54 and R^2 between 0.04 and 0.59 with the smallest values for the intermediate durations 30-360 minutes, and the largest values for the 24 and 48-hour durations. A t-test of the slope of the regression equation ($\hat{\beta}_1$) shows that the relationship with MAP can be considered significant for all durations at a significance level of 5%, except for 60-minute duration where the significance level is 7%. Estimated GLS regression models for 1-hour and 24-hour durations are shown in Figure 2. GLS regression results for all durations are summarised in Supplementary Material Table 1.

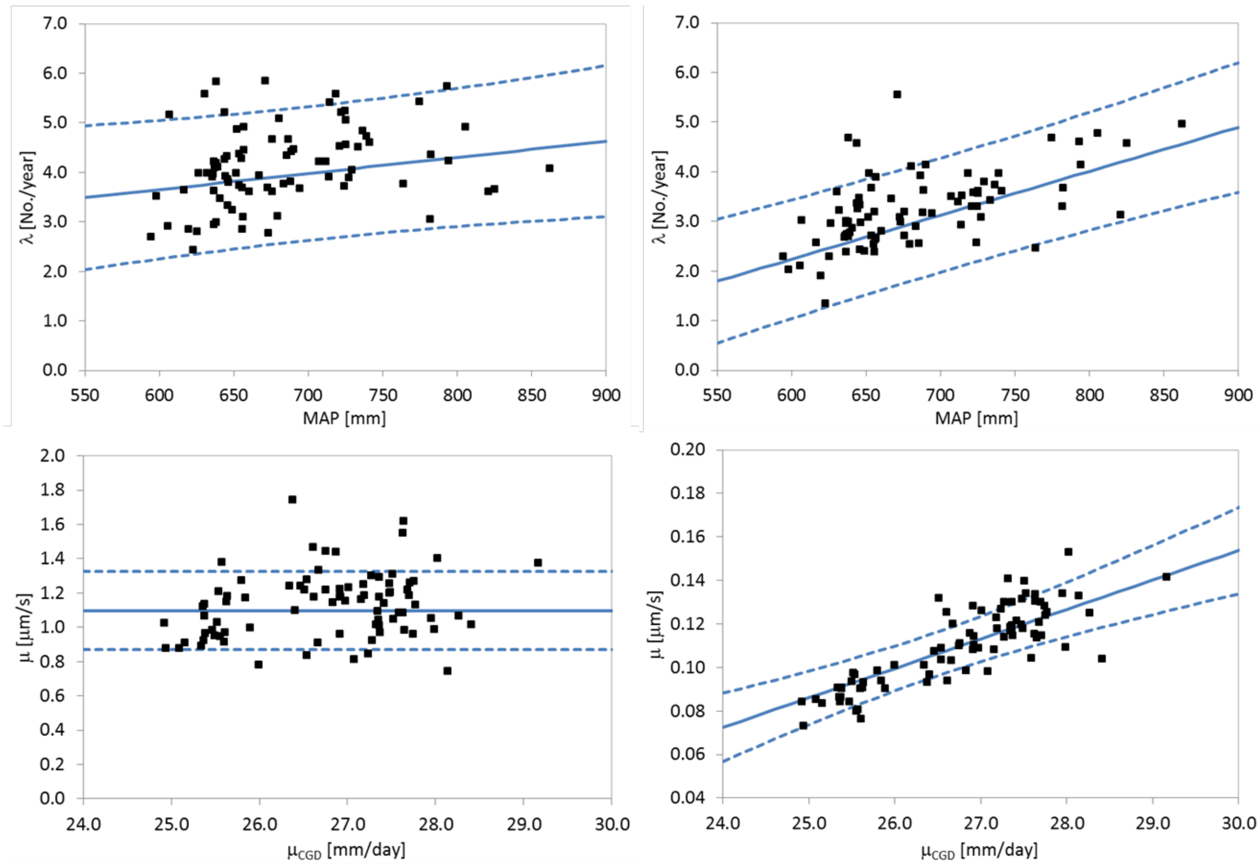

Figure 2 Regression model results. GLS regression model for the Poisson rate parameter λ with MAP as explanatory variable (top) and mean μ with μ_{CGD} as explanatory variable (bottom) for, respectively, 1-hour (left) and 24-hour (right) durations. Dotted lines represent the 95% confidence interval of the linear regression.

For the mean value of threshold exceedances μ the GLS regression results show regional variability for all durations. For durations 3-48 hours a significant part of this variability can be explained by μ_{CGD}. For these durations *RPV* ranges between 0.05 and 0.44 and R^2 between 0.17 and 0.75, and the t-test shows that the relationship with μ_{CGD} is significant at a 5% level. The largest *RPV*, R^2 and most significant slopes of the regression line are obtained for 12- and 24-hour durations. For durations smaller than 3 hours there is no clear pattern in the relationship with μ_{CGD}. For some durations significant correlations are found, whereas for other durations the correlations are not significant and even result in poorer prediction variance compared to the regional mean model (negative *RPV* for the 60-minute duration). For consistency, a regional mean model is applied for all durations smaller than 3 hours. Estimated GLS regression models for 1-hour and 24-hour durations are shown in Figure 2. GLS regression results for all durations are summarised in Supplementary Material Table 2.

For the L-CV of threshold exceedances the GLS regression results indicate regional variability for all durations except for 6 hours. No covariate information has been found to explain this variability, and a regional mean model is applied for all durations. Results are summarised in Supplementary Material Table 3.

Results of the regional model are shown in Figure 3. The figure shows estimated extreme intensities for 1 and 24-hour durations mapped on the CGD grid. It should be noted that the extreme intensities estimated from the regional model are point estimates and the maps in Figure 3 show the estimates at the grid centre points as gridded values. The explanatory variables used in the regional model are mapped on the CGD grid in Figure 3 (top row). The spatial patterns of the estimated PDS parameters λ and μ correspond to the spatial patterns of, respectively, MAP and μ_{CGD}. For durations smaller than 3 hours the regional variability is only due to the variability in λ as explained by MAP (Figure 3, middle row), whereas for durations of 3-48 hours the regional variability in μ as described by μ_{CGD} also contributes to the regional differences in the extreme intensities (Figure 3, bottom row). For smaller return periods the regional variability in λ has a relatively larger contribution to the regional variability of extreme intensities, whereas for larger return periods the regional variability in μ dominates.

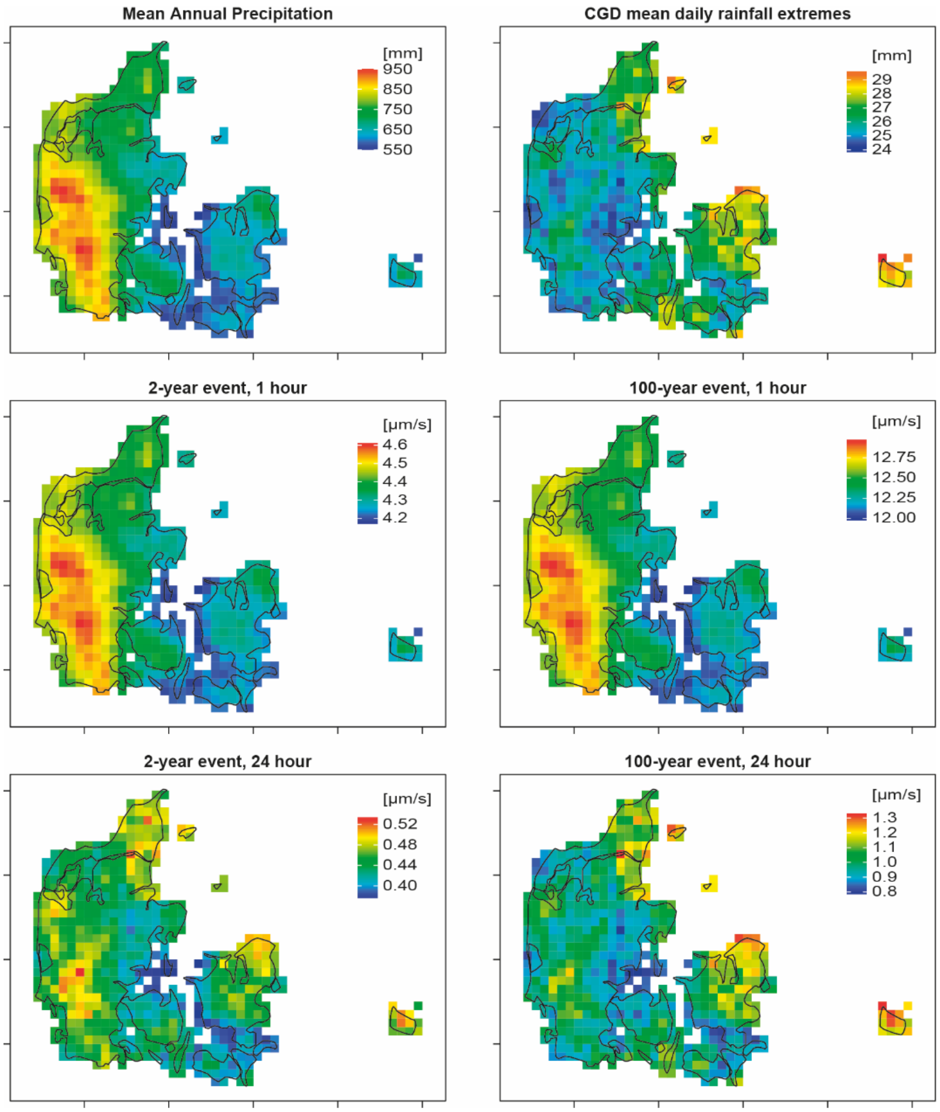

Figure 3 Regional model results. Explanatory variables of the regional model (top row): MAP (left) and μ_{GCD} (right), and estimated 2-year and 100-year intensity for 1-hour duration (middle row) and 24-hour duration (bottom row).

Figure 4 shows the range of the estimated IDF curves over Denmark for 2, 10 and 100-year return periods. The range is calculated as the minimum and maximum extreme intensity for the different durations from the CGD gridded estimates as shown in Figure 3. The relative range (range divided by the average) is smallest for durations up to 1 hour, reflecting the regional constant μ for these durations. For durations larger than 1 hour the relative range increases for increasing duration caused by an increasing regional variability of μ and λ. For 24 and 48-hour durations the upper limit of the 2 and 10-year events are similar to the lower limit of, respectively, the 10 and 100-year events.

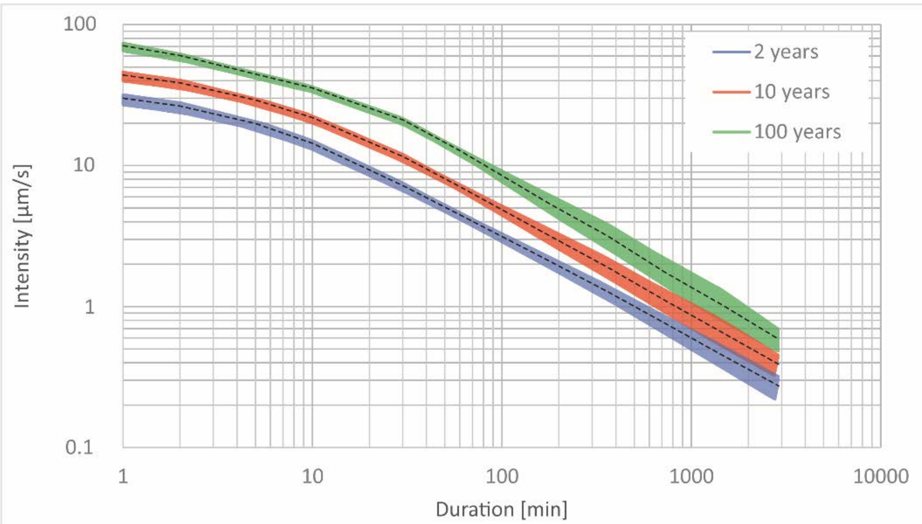

Figure 4 IDF curves for 2-year (blue), 10-year (red) and 100-year (green) events based on the regional model. The coloured areas represent the variability over Denmark, and the black dotted lines the corresponding regional averages.

Subsample analysis

To evaluate the impact of the development in data availability over time as shown in Figure 1 the subsample of 31 stations that covers almost the entire observation period has been analysed separately using the same regional modelling approach. The regional model estimated from the subsample gives, in general, smaller estimates of extreme intensities. The difference between the two models is largest for durations up to 3 hours, and larger differences are seen for larger return periods (see Figure 5). The prediction variances of the extreme intensity estimates from the regional model are smaller for the model based on the subsample. This is illustrated in Figure 6 for one location. The differences in prediction variances are largest for smaller durations and larger return periods. For 1-hour duration the uncertainty of the 2-year event estimate of the regional model based on the full sample (relative standard deviation of 8.7%) is about twofold compared to the estimate based on the subsample (4.6%), and larger differences are seen for the 100-year event estimate (23.6% and 9.2%, respectively). For the 24-hour duration the differences between the two models are smaller.

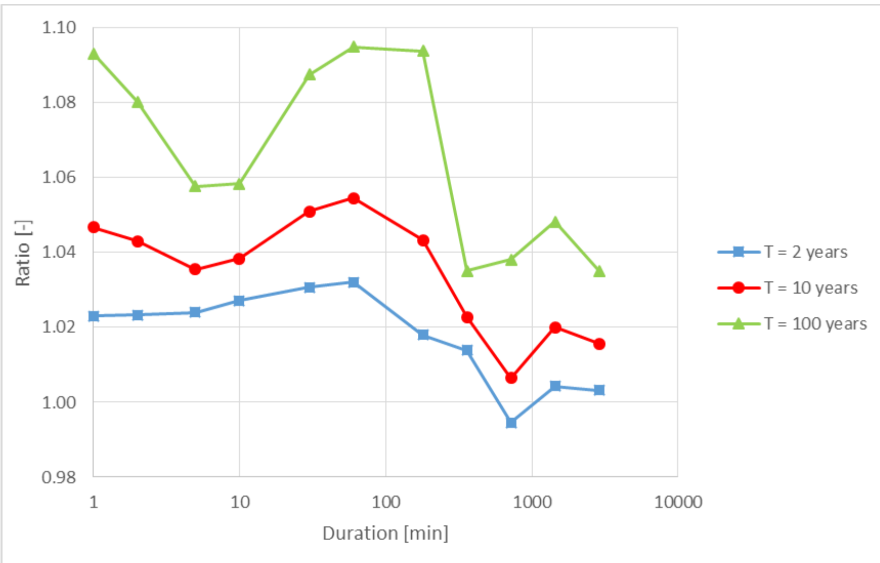

Figure 5 Ratio of regional average intensity estimates based on data from the full sample (83 stations) and the subsample (31 stations) for different durations and return periods *T*.

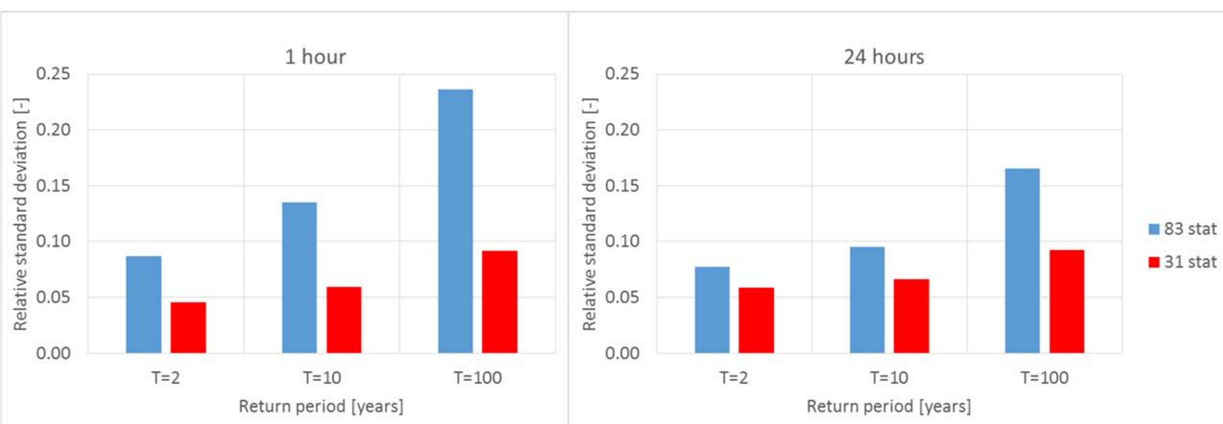

Figure 6 Relative standard deviation (standard deviation divided by intensity estimate) at a location with MAP = 632 mm and μ_{CGD} = 28.3 mm for different return periods *T* using the regional model based on data from the full sample (83 stations) and the subsample (31 stations) for 1-hour (left) and 24-hour (right) durations.

For the Poisson parameter λ GLS regression results show, in general, larger R^2 values for the subsample compared to the full sample, except for the intermediate durations 30-180 minutes. However, due to the smaller sample, the subsample has larger sampling uncertainties resulting in smaller *RPV* values for most durations. The estimated slope of the regression models are smaller for the subsample for all durations and is not significant (at a 5% level) for the durations 30-360 minutes. In general, the subsample has a smaller range of λ-estimates over Denmark and smaller prediction uncertainties. The results are summarised in Supplementary Material Table 1 and Table 4.

For the mean value of threshold exceedances μ results from the subsample analysis show that the relationship with μ_{CGD} is not significant for durations up to 3 hours where negative *RPV* values and non-significant slope estimates (at a 5% level) are obtained. For larger durations, slope estimates are significant for the subsample regressions but with smaller slope estimates (except for 12-hour duration where similar slope estimates are found). In general, the subsample results show smaller μ-estimates over Denmark. The subsample provides both smaller and larger prediction uncertainties, depending on duration, than those obtained from the full sample. The results are summarised in Supplementary Material Table 2 and Table 5.

For the shape parameter in the regional GP distribution κ larger (less negative) shape parameters are obtained for the subsample, revealing lighter-tailed GP distributions. The subsample provides smaller prediction uncertainties for durations larger than 10 minutes, except for 6-hour duration. Results are summarised in Supplementary Material Table 3.

The analysis shows larger estimates of λ and μ in the full sample, which in combination with the increase in station-years included in the regional model indicate an increasing trend in λ and μ. These results correspond well with the findings of Gregersen *et al.* (2013) who analysed a subset of the rainfall data used in this study, including 70 stations with 10–31 years of observations in the period 1979–2009. They found a significant increasing trend of λ for all durations analysed (1, 3, 6, 12 and 24 hours). Increasing trends were also found for μ for all durations, but they were statistically significant only for 1 and 3-hour durations.

Larger estimates of λ and μ, and smaller (more negative) regional GP shape parameters in the full sample all point towards larger intensity estimates as shown in Figure 5. The larger prediction uncertainties generally found for λ, μ and κ using the full sample indicate that the impact of non-stationarities is more important than the expected reduction in sampling uncertainty for increasing sample size. However, it could also reflect an increase in the spatial variability caused by adding additional stations in the analysis. It is very difficult to verify which causes are predominant due to the spatial and temporal heterogeneity of the data.

Comparison with previous studies

In the previous regional studies of Danish rainfall extremes (Madsen *et al.*, 2002; 2009) it was also found that the Poisson rate is significantly correlated with MAP. In Supplementary Material Table 4 the range of λ-estimates over Denmark from the previous studies are compared to those obtained in the current study. A general increase in λ is seen, with more pronounced increases for smaller durations. It should be noted that in the studies by Madsen *et al.* (2002, 2009) a different MAP was used based on data from the standard normal period 1961-1990 (Frich *et al.*, 1997).

The regional variability of the mean value of threshold exceedances was in the previous studies described by defining sub-regions with a constant mean. In the first study by Madsen *et al.* (2002) a larger mean intensity was seen in the Copenhagen area for durations larger than 1 hour, with differences between the western and eastern Copenhagen area for some durations. A regional model was defined with three sub-regions, respectively, (i) Copenhagen East, (ii) Copenhagen West, and (iii) the rest of the country. In the subsequent study by Madsen *et al.* (2009) the regional model was revised. For durations up to 3 hours a regional mean model was applied for the whole country, whereas for larger durations significant differences between west and east Denmark were found and two sub-regions were defined, respectively, west and east of the Great Belt. In this study new covariate information in terms of the extreme value statistic μ_{CGD} is applied. For durations 3-48 hours a significant part of the regional variability can be described by μ_{CGD}, hence allowing a more elaborate assessment of the regional variability as compared to the previous studies. For durations smaller than 3 hours, the results of the current study confirm the use of a regional mean model as in the previous studies. Regional model estimates of μ from the different studies are compared in Supplementary Material Table 5. For durations up to 1 hour a general increase in the regional mean of μ is seen. For larger durations, the range of μ over Denmark shows an increasing trend.

With respect to the L-CV the current study provides similar results as the previous study, supporting the use of a regional constant L-CV (GP shape parameter). Results from the different studies are compared in Supplementary Material Table 3. For durations up to 6 hours there is, in general, a decreasing trend towards more negative shape parameters (heavier-tailed distributions), whereas for the largest durations 24-48 hours an increasing trend (lighter-tailed distributions) is seen.

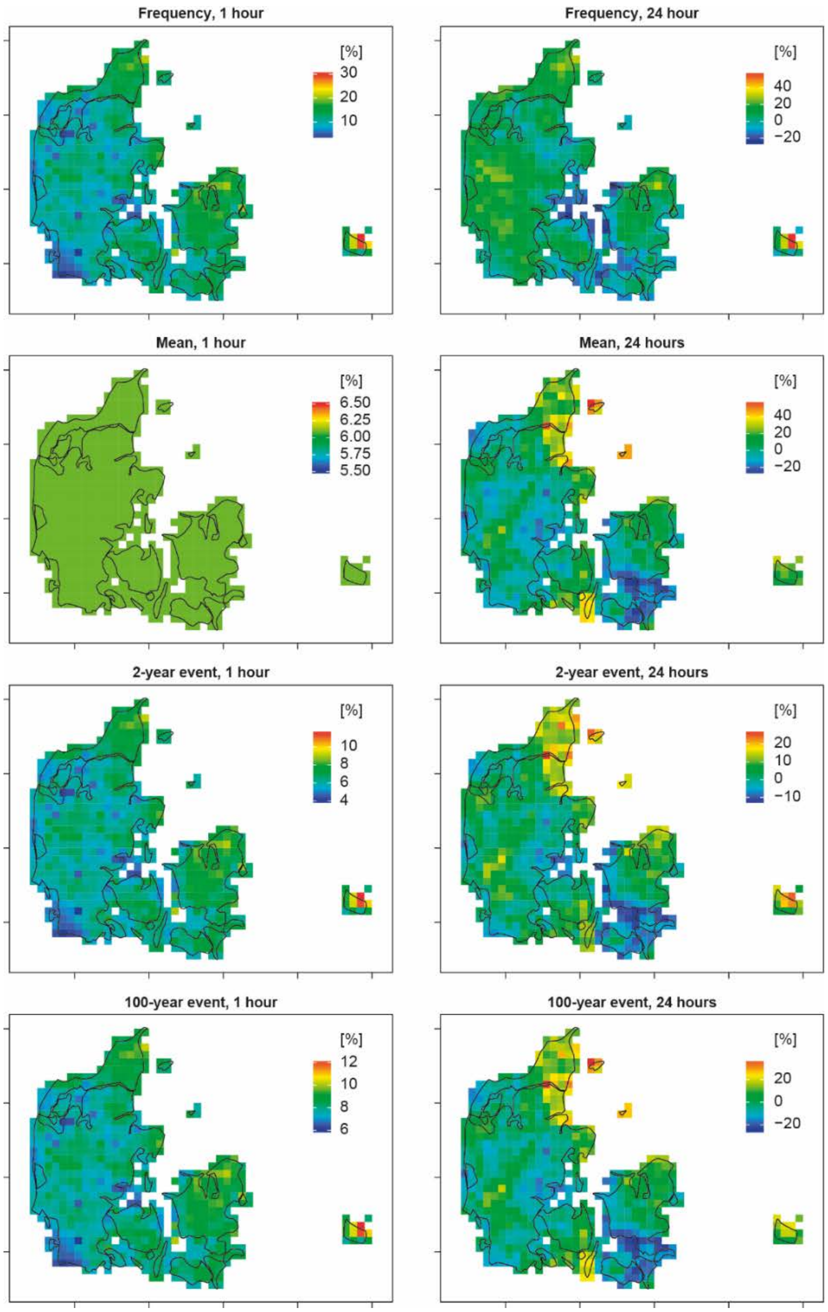

Figure 7 Differences in [%] between estimates based on the regional model in Madsen *et al.* (2009) and the new regional model for 1-hour intensity (left) and 24-hour intensity (right). The figure shows from top to bottom changes in Poisson rate (frequency), mean intensity, and 2- and 100-year intensities.

The regional model estimates of the current study and the study by Madsen *et al.* (2009) are compared in Figure 7. For the 1-hour intensity there is an increase in the Poisson rate, with a general increase from west (from about 2%) to east (up to about 30%). For the 24-hour intensity, a larger variation in the Poisson rate is seen, ranging from -25% to 58%. For the 1-hour intensity there is an increase in the mean intensity of about 6%, which is constant over Denmark since the models have a regional constant mean intensity. For the 24-hour intensity the change in mean intensity varies from -30% to 60%, with a regional pattern similar to μ_{CGD} (Figure 3, top right). For the 1-hour intensity, the changes in the extreme intensities follow the west-east pattern of the changes in the Poisson rate with an increase between 4% and 12% for the 2 and 100-year return periods. For the 24-hour intensity, the changes in the 2 and 100-year intensities follow the pattern of the changes in the mean intensity. There are both decreases and increases; from -13% to 27% for the 2-year event, and from -26% to 40% for the 100-year event. Main increases are seen in the northern part of Jutland, north-east Zealand, southern islands and Bornholm.

DISCUSSION AND CONCLUSIONS

A new regional model has been developed for estimation of IDF relationships of extreme rainfall in Denmark. The model is based on 50% more data than used in the previous regional analysis by Madsen *et al.* (2009) and uses new covariate information in terms of gridded rainfall statistics from a dense network of gauges with daily measurements (CGD). The analysis confirms previous results regarding the spatial variability of the Poisson rate; that is, the rate increases for increasing MAP for all durations analysed between 1 minute and 48 hours. With respect to the mean value of threshold exceedances μ, significant correlation with the mean extreme intensity from CGD was found for durations between 3 and 48 hours. For durations below 3 hours μ is assumed constant over Denmark in accordance with the previous studies. Finally, the analysis of L-CV of the exceedance magnitudes confirms the previous studies, and a regional constant L-CV (GP shape parameter) is applied in the model. The use of the mean extreme intensity from CGD as covariate information in the regional model allows a more elaborate assessment of the regional variability and a more consistent estimation of extreme rainfall intensities in Denmark. Based on gridded maps of μ_{CGD} and MAP the IDF relationships can be estimated at an arbitrary site in Denmark.

Compared to the previous study by Madsen *et al.* (2009) there is a general increase in extreme rainfall intensity for durations up to 1 hour caused by a general increase in the Poisson rate and the mean extreme intensity and a more negative GP shape parameter. For larger durations both increases and decreases are seen due to the correlation with μ_{CGD} compared to the division into two regions with constant mean extreme intensity in the previous study.

To analyse the impacts of using the temporal heterogeneous dataset a subsample analysis was conducted including only stations that cover almost the entire observation period. The analysis showed that the relatively larger contribution of station-years in recent years combined with increases in λ and μ and decreasing (more negative) GP shape parameters give larger estimates of extreme intensities compared to including only records that cover the full observation period in the regional model. The regional model based on the full sample has larger prediction uncertainty of intensity estimates than the model based on the subsample. This is due to the non-stationarities in the data but may also reflect larger spatial variability in the full sample.

Gregersen *et al.* (2015) analysed long records of daily rainfall dating back to 1874 and found a general increase in the Poisson rate but overlaid by a multi-decadal variability that indicated a cyclic behaviour. The increase seen in recent years is much larger than the long-term trend but may, at least to some extent, be attributed to the multi-decadal variability seen in the long records. Since it is currently not possible to attribute the recent increases to anthropogenic changes or natural variability, the regional model using the full sample provides the best estimate according to current knowledge of extreme rainfall characteristics and associated uncertainties. Rather than including the non-stationarities in the regional model implicitly as an additional source of uncertainty, a model that explicitly describes non-stationarities in the PDS parameters could be developed. This is currently being investigated.

ACKNOWLEDGEMENTS

This work was carried out with the support of The Foundation for Development of Technology in the Danish Water Sector, contract no. 7492-2012, and the Danish Council for Strategic Research as part of the RiskChange project, contract no. 0603-00390 (http://riskchange.dhigroup.com).

REFERENCES

Alila Y. 1999 A hierarchical approach for the regionalization of precipitation annual maxima in Canada. *J. Geophys. Res.*, **104**(D24), 31,645–31,655.

Arnbjerg-Nielsen K., Willems P., Olsson J., Beecham S., Pathirana A., Gregersen I.B., Madsen H. & Nguyen V.-T.-V. 2013 Impacts of climate change on rainfall extremes and urban drainage systems: a review. *Water Sci. Technol.*, **68(**1), 16-28. doi: 10.2166/wst.2013.251

Beguería S. & Vicente-Serrano S.M. 2006 Mapping the hazard of extreme rainfall by peaks over threshold extreme value analysis and spatial regression techniques. *J. Appl. Meteorol. Climatol.* , **45**, 108-124.

Burn D.H. 1990 Evaluation of regional flood frequency analysis with a region of influence approach. *Water Resour. Res.*, **26**(10), 2257–2265.

Burn D.H. 2014 A framework for regional estimation of intensity–duration–frequency (IDF) curves. *Hydrol. Process.*, **28**, 4209–4218.

Di Baldassarre G., Castellarin A. & Brath A. 2006 Relationships between statistics of rainfall extremes and mean annual precipitation: an application for design-storm estimation in northern central Italy. *Hydrol. Earth Syst. Sci.*, **10**, 589–601.

Frich P., Rosenørn S., Madsen H. & Jensen J.J. 1997 *Observed precipitation in Denmark, 1961–1990*. Technical report 97-8. Danish Meteorological Institute, Ministry of Transport. Copenhagen, Denmark.

Gaál L., Kyselý J. & Szolgay J. 2008 Region-of-influence approach to a frequency analysis of heavy precipitation in Slovakia. *Hydrol. Earth Syst. Sci.*, **12**, 825–839.

Gregersen I.B., Sørup H.J.D., Madsen H., Rosbjerg D., Mikkelsen P.S. & Arnbjerg-Nielsen K. 2013 Assessing future climatic changes of rainfall extremes at small spatio-temporal scales. *Clim. Change*, **118**(3-4), 783-797.

Gregersen I.B., Madsen H., Rosbjerg D. & Arnbjerg-Nielsen K. 2015. Long term variations of extreme rainfall in Denmark and southern Sweden. *Clim. Dyn.*, **44**, 3155-3169, DOI 10.1007/s00382-014-2276-4.

Haddad K., Rahman A. & Green J 2011 Design rainfall estimation in Australia: a case study using L moments and Generalized Least Squares Regression. *Stoch. Env. Res. Risk Assess.*, **25**, 815–825.

Hosking J.R.M. & Wallis, J.R. 1993 Some statistics useful in regional frequency analysis. *Water Resour. Res.*, **29**(2), 271–281. Correction, *Water Resour. Res.*, **31**(1), 251.

Hosking J.R.M. & Wallis J.R. 1997 *Regional Frequency Analysis: An Approach Based on L-moments*. Cambridge University Press, Cambridge, UK.

Jørgensen H.K., Rosenørn S., Madsen H. & Mikkelsen, P.S. 1998 Quality control of rain data used for urban runoff systems. *Water Sci. Technol.*, **37**(11), 113-120.

Kyselý J., Gaál L. & Picek J. 2011 Comparison of regional and at-site approaches to modelling probabilities of heavy precipitation. *Int. J. Climatol.*, **31**, 1457–1472.

Madsen H. & Rosbjerg D. 1997a The partial duration series method in regional index-flood modelling. *Water Resour. Res.*, **33**(4), 737-746.

Madsen H. & Rosbjerg D. 1997b Generalized least squares and empirical Bayes estimation in regional partial duration series index-flood modelling. *Water Resour. Res.*, **33**(4), 771-781.

Madsen H., Pearson C.P. & Rosbjerg D. 1997 Comparison of annual maximum series and partial du-ration series methods for modeling extreme hydrologic events, 2. Regional modelling. *Water Resour. Res.*, **33**(4), 759-769.

Madsen H., Mikkelsen P.S., Rosbjerg D. & Harremoës P. 2002 Regional estimation of rainfall-intensity-duration-frequency curves using generalised least squares regression of partial duration series statistics. *Water Resour. Res.*, **38**(11), 1239, doi: 10.1029/2001WR001125.

Madsen H., Arnbjerg-Nielsen K. & Mikkelsen P. S. 2009 Update of regional intensity-duration-frequency curves in Denmark: Tendency towards increased storm intensities. *Atm. Res.*, **92**(3), 343-349.

Reis Jr. D., Stedinger J. & Martins E. 2004 Operational Bayesian GLS regression for regional hydrologic analyses. Proceedings: Critical Transitions in Water and Environmental Resources Management, 1-10, doi: 10.1061/40737(2004)284

Scharling M. 1999 Klimagrid Danmark nedbør *10x10km* (*Ver. 2*), *(in Danish, Climate Grid Denmark precipitation 10x10km (version 2)),* Technical report 99-15. Danish Meteorological Institute, Ministry of Transport, Copenhagen, Denmark.

Scharling M. 2012 *Climate Grid Denmark - Dataset of use in research and education - Daily and monthly values 1989-2010*. Technical report 12-10. Danish Meteorological Institute, Ministry of Climate and Energy, Copenhagen, Denmark.

Schilling W. 1991 Rainfall data for urban hydrology: what do we need? *Atm. Res.*, **27**, 5–22. DOI: 10.1016/0169-8095(91)90003-F

Smithers J.C. & Schulze R.E. 2001 A methodology for the estimation of short duration design storms in South Africa using a regional approach based on L-moments. *J. Hydrol.*, **241**, 42–52.

Stedinger J.R. & Tasker G.D. 1985 Regional Hydrologic Analysis. 1. Ordinary, weighted, and generalized least-squares compared. *Water Resour. Res.*, **21**(9), 1421-1432.

Wallis J.R., Schaefer M.G., Barker B.L. & Taylor G.H. 2007 Regional precipitation-frequency analysis and spatial mapping for 24-hour and 2-hour durations for Washington State. *Hydrol. Earth Syst. Sci.*, **11**, 415-442.

SUPPLEMENTARY MATERIAL

Table 1 GLS regression results for the Poisson rate parameter λ using MAP as explanatory variable. Reduction in average prediction variance *RPV*, pseudo R^2, estimated slope of regression equation $\boldsymbol{\hat{\beta}_1}$ (10^{-3} years^{-1}/mm) with corresponding standard deviation (10^{-3} years^{-1}/mm) in parenthesis, and t-test significance level α.

Duration [min]	83 stations				31 stations			
	RPV	R^2	$\hat{\beta}_1$	α	*RPV*	R^2	$\hat{\beta}_1$	α
1	0.24	0.27	7.29 (1.64)	< 0.001	0.23	0.31	4.55 (1.57)	0.005
2	0.19	0.22	6.63 (1.68)	< 0.001	0.27	0.40	4.08 (1.37)	0.004
5	0.13	0.16	5.49 (1.69)	0.002	0.10	0.21	2.89 (1.38)	0.04
10	0.10	0.13	5.88 (1.91)	0.003	0.09	0.18	3.29 (1.55)	0.04
30	0.06	0.08	4.34 (1.77)	0.02	-0.04	0.04	1.99 (1.53)	0.20
60	0.01	0.04	3.26 (1.80)	0.07	-0.08	0	1.39 (1.59)	0.38
180	0.02	0.05	3.35 (1.66)	0.05	-0.07	0	1.48 (1.67)	0.38
360	0.06	0.09	4.36 (1.63)	0.009	0.02	0.09	2.91 (1.63)	0.08
720	0.11	0.15	5.52 (1.60)	0.001	0.15	0.23	4.25 (1.56)	0.008
1440	0.30	0.33	8.85 (1.58)	< 0.001	0.46	0.55	7.39 (1.50)	< 0.001
2880	0.54	0.59	12.4 (1.47)	< 0.001	0.66	0.73	11.0 (1.61)	< 0.001

Table 2 GLS regression results for the mean μ using μ_{CGD} as explanatory variable. Reduction in average prediction variance *RPV*, pseudo R^2, estimated slope of regression equation $\hat{\boldsymbol{\beta}}_1$ (μm/s/mm) with corresponding standard deviation (μm/s/mm) in parenthesis, and t-test significance level α.

Duration [min]	83 stations				31 stations			
	RPV	R^2	$\hat{\beta}_1$	α	*RPV*	R^2	$\hat{\beta}_1$	α
1	0.01	0.08	2.09E-01 (1.20E-01)	0.09	-0.10	0	1.53E-01 (1.63E-01)	0.35
2	0.05	0.15	2.13E-01 (1.08E-01)	0.05	-0.11	0.01	1.54E-01 (1.47E-01)	0.30
5	0.16	0.28	2.17E-01 (8.72E-02)	0.01	-0.02	0.17	1.80E-01 (1.17E-01)	0.13
10	0.04	0.15	1.28E-01 (6.55E-02)	0.06	-0.43	0.01	8.18E-02 (8.12E-02)	0.32
30	0.05	0.12	9.12E-02 (4.14E-02)	0.03	-0.34	0	2.71E-02 (5.02E-02)	0.59
60	-0.03	0.04	4.26E-02 (2.81E-02)	0.13	-0.46	0	2.10E-03 (3.22E-02)	0.95
180	0.05	0.17	3.33E-02 (1.28E-02)	0.01	-0.09	0.25	2.89E-02 (1.60E-02)	0.07
360	0.13	0.25	2.77E-02 (8.10E-03)	0.001	0.01	0.39	2.29E-02 (9.90E-03)	0.02
720	0.31	0.60	1.94E-02 (4.41E-03)	< 0.001	0.40	1.00	1.95E-02 (5.80E-03)	0.001
1440	0.44	0.75	1.35E-02 (2.42E-03)	< 0.001	0.26	0.79	1.09E-02 (3.34E-03)	0.002
2880	0.13	0.27	5.26E-03 (1.45E-03)	< 0.001	-0.06	0.40	3.75E-03 (1.88E-03)	0.05

Table 3 GLS regression results for the shape parameter κ. Regional estimate of GP shape parameter and corresponding standard deviation in parenthesis for current and previous studies.

Duration [min]	1979-2012 (83 stations)	1979-2012 (31 stations)	1979-2005[1] (66 stations)	1979-1997[2] (41 stations)
1	-0.158 (0.0767)	-0.125 (0.0591)	-0.152 (0.104)	-0.132 (0.103)
2	-0.110 (0.0681)	-0.0803 (0.0740)	-0.0971 (0.0621)	-0.101 (0.136)
5	-0.0743 (0.0399)	-0.0549 (0.0609)	-0.0769 (0.0209)	-0.0616 (0.0965)
10	-0.122 (0.0417)	-0.107 (0.0615)	-0.116 (0.0410)	-0.0620 (0.0286)
30	-0.207 (0.0500)	-0.185 (0.0193)	-0.200 (0.0350)	-0.165 (0.0274)
60	-0.207 (0.0733)	-0.182 (0.0267)	-0.205 (0.0615)	-0.134 (0.0309)
180	-0.175 (0.0768)	-0.140 (0.0248)	-0.170 (0.0333)	-0.0806 (0.0395)
360	-0.180 (0.0233)	-0.174 (0.0259)	-0.189 (0.0628)	-0.155 (0.0427)
720	-0.137 (0.0680)	-0.107 (0.0596)	-0.145 (0.0658)	-0.134 (0.0495)
1440	-0.124 (0.0644)	-0.103 (0.0299)	-0.149 (0.0945)	-0.169 (0.0479)
2880	-0.0894 (0.0681)	-0.0754 (0.0325)	-0.105 (0.0910)	-0.106 (0.109)

[1]Madsen *et al.* (2009), [2]Madsen *et al.* (2002)

Table 4 Range over Denmark of Poisson rate parameter λ (years^{-1}) and corresponding standard deviation in parenthesis (years^{-1}) with MAP as explanatory variable for current and previous studies.

Duration [min]	1979-2012 (83 station)	1979-2012 (31 stations)	1979-2005[1] (66 stations)	1979-1997[2] (41 stations)
1	3.13 – 6.10 (0.628 – 0.752)	3.43 – 5.29 (0.406 – 0.571)	2.74 – 5.35 (0.539 – 0.614)	2.63 – 4.36 (0.482 – 0.609)
2	3.23 – 5.93 (0.658 – 0.784)	3.50 – 5.16 (0.314 – 0.467)	2.82 – 5.02 (0.528 – 0.599)	2.60 – 4.21 (0.280 – 0.406)
5	3.27 – 5.50 (0.661 – 0.786)	3.51 – 4.69 (0.324 – 0.475)	2.73 – 4.77 (0.540 – 0.610)	2.36 – 4.00 (0.323 – 0.436)
10	3.62 – 6.01 (0.756 – 0.897)	3.86 – 5.20 (0.378 – 0.543)	3.09 – 5.12 (0.557 – 0.629)	2.63 – 4.30 (0.398 – 0.512)
30	3.43 – 5.19 (0.678 – 0.811)	3.68 – 4.49 (0.379 – 0.540)	2.88 – 4.57 (0.568 – 0.640)	2.43 – 4.30 (0.471 – 0.586)
60	3.47 – 4.79 (0.675 – 0.811)	3.64 – 4.21 (0.394 – 0.560)	2.88 – 4.42 (0.583 – 0.655)	2.50 – 4.16 (0.478 – 0.592)
180	3.02 – 4.39 (0.590 – 0.719)	3.26 – 3.86 (0.436 – 0.604)	2.77 – 4.15 (0.562 – 0.636)	2.56 – 3.82 (0.464 – 0.576)
360	2.56 – 4.33 (0.591 – 0.716)	2.77 – 3.96 (0.433 – 0.594)	2.32 – 4.07 (0.511 – 0.579)	2.16 – 4.00 (0.350 – 0.442)
720	2.08 – 4.33 (0.593 – 0.713)	2.26 – 3.99 (0.422 – 0.575)	1.82 – 3.85 (0.481 – 0.548)	1.66 – 4.11 (0.285 – 0.377)
1440	1.74 – 5.35 (0.574 – 0.695)	2.02 – 5.03 (0.395 – 0.543)	1.63 – 4.62 (0.513 – 0.573)	1.31 – 5.01 (0.318 – 0.408)
2880	1.57 – 6.61 (0.498 – 0.614)	1.87 – 6.34 (0.436 – 0.594)	1.67 – 5.94 (0.482 – 0.538)	1.40 – 5.88 (0.354 – 0.453)

[1]Madsen *et al.* (2009), [2]Madsen *et al.* (2002)

Table 5 Range over Denmark of mean μ (µm/s) and corresponding standard deviation in parenthesis (µm/s) for current study using μ_{CGD} as explanatory variable and previous studies based on sub-regional divisions.

Duration [min]	1979-2012 (83 station)	1979-2012 (31 stations)	1979-2005[1] (66 stations)	1979-1997[2] (41 stations)
1	6.22 (0.491)	6.03 (0.520)	5.97 (0.368)	5.85 (0.766)
2	5.99 (0.380)	5.84 (0.418)	5.78 (0.345)	5.47 (0.689)
5	4.90 (0.295)	4.80 (0.286)	4.71 (0.191)	4.54 (0.541)
10	3.58 (0.225)	3.49 (0.124)	3.45 (0.129)	3.33 (0.110)
30	1.82 (0.165)	1.76 (0.102)	1.74 (0.0572)	1.61 (0.0551)
60	1.10 (0.114)	1.05 (0.0582)	1.03 (0.0464)	0.948 (0.0354)
180	0.410 – 0.608 (0.0386 – 0.0595)	0.405 – 0.577 (0.0286 – 0.0658)	0.466 (0.0188)	0.432 – 0.517 (0.0246 – 0.0757)
360	0.222 – 0.387 (0.0247 – 0.0377)	0.224 – 0.360 (0.0172 – 0.0405)	0.263 – 0.292 (0.0244 – 0.0279)	0.257 – 0.340 (0.0181 – 0.0479)
720	0.128 – 0.243 (0.00956 – 0.0180)	0.130 – 0.246 (0.00775 – 0.0230)	0.167 – 0.183 (0.0203 – 0.0277)	0.162 – 0.234 (0.0130 – 0.0284)
1440	0.0725 – 0.153 (0.00505 – 0.00980)	0.0757 – 0.140 (0.00526 – 0.0136)	0.0921 – 0.115 (0.00755 – 0.0151)	0.0940 – 0.131 (0.00872 – 0.0218)
2880	0.0489 – 0.0802 (0.00460 – 0.00690)	0.0507 – 0.0730 (0.00381 – 0.00810)	0.0551 – 0.0700 (0.00436 – 0.00834)	0.0581 – 0.0756 (0.00499 – 0.0127)

[1]Madsen *et al.* (2009), [2]Madsen *et al.* (2002)

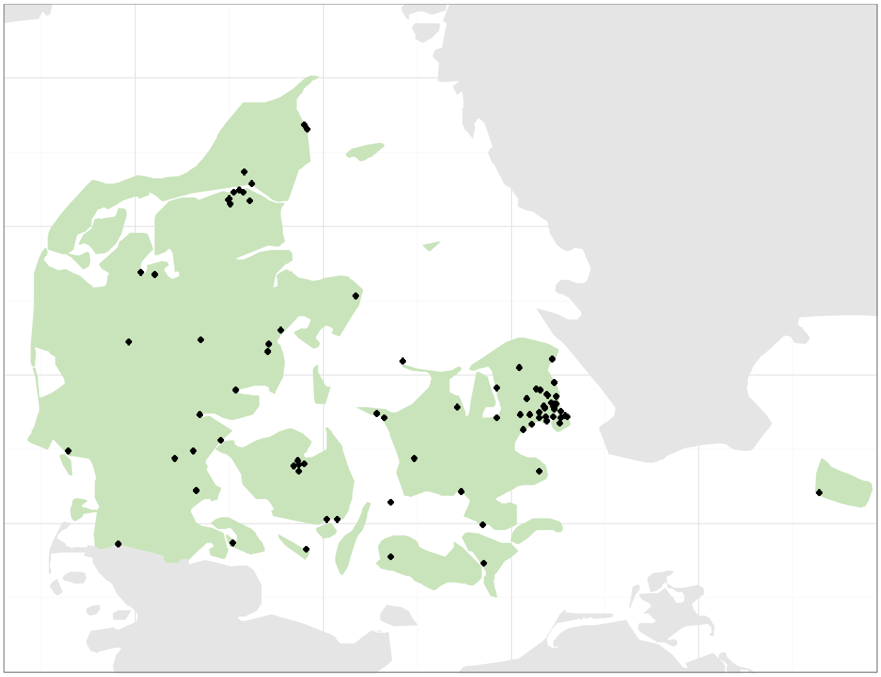

Figure 1 Location of the high-resolution rain gauges used in the study.